A new approach to simulate coating thickness in cold spray

Hongjian Wu, Xinliang Xie, Meimei Liu, Chaoyue Chen, Hanlin Liao, Yicha Zhang, Sihao Deng

A New Approach to Simulate Coating Thickness in Cold Spray

Hongjian WU [a], Xinliang XIE [a], Meimei LIU [a], Chaoyue CHEN [b], Hanlin LIAO [a], Yicha ZHANG [c], Sihao DENG [a*]

a. ICB-PMDM-LERMPS UMR 6303, CNRS, UTBM, Université de Bourgogne Franche-Comté, 90010 Belfort, France

b. State Key Laboratory of Advanced Special Steels, School of Materials Science and Engineering, Shanghai University, Shanghai 200444, China

c. ICB-COMM UMR 6303, CNRS, UTBM, Université de Bourgogne Franche-Comté, 90010 Belfort, France

* Corresponding author: sihao.deng@utbm.fr (Sihao DENG)

Abstract: In the process of cold spray on complex components, the coating thickness is an important indicator to monitor and control. Current methods such as destructive tests or direct mechanical measurements can only be performed after spraying as an afterthought. Moreover, these methods lead to production shutdown and additional costs obviously. This article presents a novel approach predicting coating thickness for components with complex curved surfaces, especially in the case of shadow effects. Firstly, a three-dimensional geometric model of the coating profile based on Gaussian distribution was developed. In addition, the relative deposition efficiency (RDE) resulting from the different robot kinematic parameters was illustrated in detail. Secondly, this model is coupled with robotic trajectories and processing parameters to simulate coating deposition in robotic off-line programming software. Finally, the coating morphologies as well as the predicted coating thickness are presented in a graphical virtual environment. According to the results of the simulation, the robot trajectory, operating parameters and spray strategy can be adjusted with iteration in the feedback loop to achieve the desired coating thickness distribution. Both numerical and experimental verifications were carried out in the end of this study. The results show that this proposed method has a good prediction accuracy for practice.

Keywords: Coating thickness model; Simulation; Shadow effects; Relative deposition efficiency; Cold spray; Robot

1. Introduction

Cold spraying (CS) is a solid-state material deposition technique, which can prepare a variety of functional coatings as a spray process for applications in surface technology [1–4]. CS has many advantages that make the technology potentially very competitive in the manufacturing industry for durable products. In particular, high deposition rates and efficiencies make this surface technology efficient for additive manufacturing and structural repairing[5–8]. Generally, cold sprayed coating is produced by the motion of spraying gun, controlled by industrial robotic. Researchers have already used the robot off-line programming (OLP) technique in a graphical virtual environment to replace the programming by teaching on the real spray robot in the site, which makes the CS process more automatic and intelligent[9,10].

Nowadays, various spray coatings for complex components such as turbine blades and vanes have very exacting demands for the distribution of thickness. Meeting the requirements of coating thickness distribution is critical for the performance and the service life of components. Traditionally, the desired coating thickness has been provided by trial and error method. In this process, there are many methods for testing the coating thickness, such as destructive tests or direct mechanical measurements. However, they are all performed after spraying as an afterthought, which makes those approaches in most cases time-consuming and leads to higher costs. In order to simplify and speed up the coating development, simulation technology for CS processes was proposed and developed, particularly for component-based simulations that concern coating-thickness distributions, heat and stress distributions et al. For example, Ju et al.[11] developed a continuous micro mechanic model for depicting the interplay relating heat, solidifying pattern and stress/strain curve, so that thermo-mechanic actions and residual stress can be forecasted in spraying processes. Liu et al.[12] studied the heat and mechanic behaviors of plasma sprayed coatings during fabricating by developing a 3D multilayer model. However, the objective of coating thickness simulation is to optimize the robot trajectory so that the coating can be evenly deposited on the surface of the substrate or variably deposited on different regions of a specified surface as required, e.g. coating turbine blades with diverse thicknesses. According to the simulation results, coating properties, such as coating thicknesses, porosities, interface roughnesses and even residual stresses, can be predicted. For simulation-based prediction, there are a set of proposed methods in the literature. Duncan et al.[13] optimized the robot path by creating the required coat thickness over the surface. They proposed a flow rate distribution function to describe the behavior of the nozzle, and the coating deposition was represented by mass, which was counted by multiplying a mass flow rate and working time with a flow rate distribution formula. Base on the model proposed by Duncan, Kout, et al.[14] aimed to search a successive time-dependent array of nozzle configuration for creating the desired coating thickness. The difference of the newly proposed method was that the coating deposition was represented by its highness, which was counted by multiplication of volume flow rate with flow rate distribution formula. However, they all did not consider the actual robot kinematics parameters in their model, such as spray distances and spray angles, which are key factors of the deposition efficiency (DE) and result

in the coating. Sadovoy et al.[9] developed a self-constant model based on mass conservation principle. This model considers the effects of the actual processing parameters and spraying conditions. However, it only involves the influence of the spray angles as a single processing parameter on the profile of the coating. The effect of other processing parameters, e.g., the spray distances and the nozzle travel speeds were not investigated. Cai et al [15] employed a symmetric Gaussian distribution curve to characterize the single-coat profile. They proposed a concept of flatness to illustrate their homogeneity coating thickness. However, they did not expand to 3 dimensions to explain the flatness of the coating. To fix this problem, C. Chen et al [16] proposed a numeral model of the single coat profile to discuss the effects of gun turn angle, nozzle pass speed, and scanning step on the cold sprayed coating thickness distribution. However, their model excluded the consideration of the impact of spray distance. Wiederkehr et al. [17] reported a method to obtain a 3D flow distribution model by testing coating profiles, which acquired from spraying onto surfaces with a stationary nozzle. However, the analysis was limited to the case of flat surfaces and did not involve other more complicated situations, e.g., curved surfaces. Djurić et al.[18] presented a self-consistent way for counting the mass rate distribution function, efficiency, and cone angle during spraying. They simulated the space mass flux distribution generated out of the nozzle by developing a spraying deposition model. However, there were no explanations of application examples to validate the model in their report. In Stepanenko [19] report, a method was developed to compute feed rate control laws, which can provide production of uniform coating-thicknesses or coating-thickness variation predefined laws. Besides, Hansbo et al [20] proposed a spraying cone model to optimize the coating-thickness for rotationally symmetric components. However, this model was not validated for coating complex components where concave surface features may exist. Chen et al. [21] used an FEA (finite element analysis) model to simulate transient coating accumulated processes and heat evolutions during cold spraying. However, using finite element analysis or numerical methods to simulate the coating deposition process, such as ANSYS and MATLAB, it always requires meshing the workpiece, and then calculates the coating thickness and assigns the final result to each node of the grid. As the nozzle moves, the coating thickness of each node will be continuously updated. Therefore, this approach must be based on the same dimension and continuous grid and cost much computation. For those substrates with a large radius of curvature or discontinuous surface regions, it would not be suitable.

Based on the reviewed works above, it is easy to conclude that most of the coating-thickness simulations mainly focus on the development of coating-thickness models. The experimental process is generally an operation of numerical model superposition, for which it is difficult to show the behavior of coating stack and the macroscopic appearance of final coating distributions intuitively. Besides, the calculation of the coating thickness should not be just a simple addition of specific numerical value because the physical processes involved in coating deposition are very complex. DE impacted by the different parameters should not be ignored. Most notably, there are still no effective ways to simulate and predict the coating thickness distribution on complex surfaces with a ‘shadow

effect'. Shadow effect means that some convex features on the substrate obstruct the flight path of particles to other convex or concave shapes, which is illustrated in Fig. 1.

To simulate the coating in the 'shadow effect' condition so as to better optimize the coating process, in this study, a new simulation approach is proposed. This method uses a numerical model of coating profile based on Gaussian distribution to construct a real-time evolving 3D profile geometric model on the coating substrate. Based on this evolving model, the 'shadow effect' can be predicted and evaluated.

The remaining of the paper is organized as follows: the second section described the principle of creating a single coating thickness model as well as a continuous coating thickness model. At the same time, the RDE, which is determined by robot kinematic parameters, as spray angles, spray distances and nozzle traverse speed, was illustrated in detail; the third section mainly introduced the process of coating thickness simulation using the developed model. All of the operations are integrated into the ''thermal spraying toolkit'' (TST)[10], a home-made software package, and then displayed on the graphic interface of RobotStudio™; finally, the simulation results and assumptions by a flat and a 'shading effect' workpiece were discussed and verified in the corresponding experiments.

2. Coating deposition model

2.1. Single coating profile model

The model describing the feedstock jet distribution out of the nozzle is essential for calculation of coating-thickness distribution. For the coating deposited by CS process, the coating-thickness distribution also known as coating profile can be expressed by a Gaussian approximation as in the equation below [15,16]:

$$\varphi = \zeta(\theta)\int_0^T \left(\int \frac{A}{\sigma\sqrt{2\pi}} e^{-\left(\frac{(x-\mu_x)^2}{2\sigma^2}+\frac{(y-\mu_y)^2}{2\sigma^2}\right)} dxdy\right)dt \qquad (1)$$

The amplitude factor is expressed by A, which is related to the actual feedstock flow rate. The standard deviation of the coating-profile is represented as σ, which is linked to spraying cone angles as well as distances. The center coordinate of coating-profile on the substrate can be described as (μx, μy). ζ(θ) is the DE as a function of spray angle. Each variable value can be got by experimental investigation.

The model proposed by Chen [16], which was illustrated in 2-dimensional polar coordinates, is a typical representative. In difference to that, in this paper, the model is described in a three-dimensional Cartesian coordinate system. As shown in Fig.2, the nozzle is defined as a point in the Cartesian coordinate system. The angle of incidence, i.e. spray angle, is θ (on *X*-*Y* plane). In the *YZ*

plane, the spray cone in the Cartesian coordinate system is divided into a series of rays with a constant interval angle. Exemplary rays, as dash lines in Fig.2. For perpendicular spray case, the coating profile is conical and symmetric with the central line of the nozzle. Thus, the spray length at the same deflection angle is constant. For example at the deflection angle of ψ as indicated in Fig.2, the spray length *AB* has the same value as *ab*. And the angle between these two rays is γ. Besides, due to the fact that mass distribution out of the nozzle is constant, it can assume that the spray length at each deflection angle is constant during inclination. For example, when the *XY* plane rotates around the x-axis (now the spray angle is β on the *X1-Y1* plane), as indicated in Fig.2, the spray length *AB* has the same value as *CD*

In computer graphics and computational physics applications, an object can be represented by a three-element vector, which typically is used to describe a position, normal and Euler rotation. In addition, a transformation (rotation and translation) can be described by a matrix from a three-element vector and a quaternion. In order to express the coating profile model in a three-dimensional graphics environment while maximally preserve the characteristics of the spraying, the following assumptions are proposed in this study: firstly, powders are stably ejected from the nozzle and deposited on the surface of the workpiece during the motion of the nozzle. Therefore, these particles can be considered as a finite number of rays sharing the same starting point. As shown in Fig. 3a and Fig. 3d, these rays are obtained by rotation and symmetric operation of the centerline, and they will intersect the substrate to create intersections. In this way, the effective area will be determined for creating a coating profile. Secondly, a single coating profile consists of a finite number of cylinders with the same diameter, and the height of each cylinder equals the value of the corresponding Gaussian function. As shown in Fig. 3b and Fig. 3e, based on the intersection, circles will be created and stretched in the opposite direction of the ray to form a cylinder. The distance stretched is equal to the spray length. The smaller the radius of the cylinder is, the higher the accuracy of the simulation results will be. However, the calculation time will also be longer. This study uses a cylinder with a radius of 0.02 mm. The cylinders are established only where the rays touch. Therefore, the coating profile can be in a myriad of shapes, even non-continuous (As displayed in Fig. 3c and Fig. 3f).

2.2. Continuous coating profile model

Normally, a set of continuous random variables can be discretized according to certain rules. In order to simulate the deposited coatings on the substrate during the nozzle motion, we assume that the continuous coating profile is a collection of single coating profiles. As Fig. 4 displays, by selecting the appropriate distance between two discrete points, it can acquire the coating distribution model deposited on the substrate under traveling of the nozzle. According to calculations, as long as the distance is less than σ, a continuous coating profile closed to the actual situation can be obtained. In this study, the distance between two discrete points equals σ/2.

In three-dimensional graphics environment, as shown in Fig. 5a, the first single coating profile will be created on the substrate, Then the second single coating profile will be created on the substrate and overlaps with the first single coating profile, and so forth. Finally, continuous coating topography can be created on any topographic substrate, like flat in Fig. 5b, curved surface in Fig. 5c and complex surface in Fig. 5d.

2.3. Effects analysis of the different robot kinematic parameters

The robot kinematics behavior is quite significant to ensure the required quality of the coating. The main motion parameters during the spraying process include spray angle, spray distance and nozzle traverse speed. They change the coating profile by affecting the DE. Gilmore et al.[22] defined it as the rate of the mass of the deposited particles to the overall mass of the spray particles. In practice, DE is a systematic variable, and the influencing factors involved are very complicated. Among them, the deposition behaviors and deposition mechanisms of particle play an important role. Nowadays, substantial research has been carried out to understand the deposition of particle. For example, Assadi et al.[23,24] proposed that the occurrence of bonding can be illustrated by shear instability. Li et al.[25] examined the effects of spray angle and particle size on the critical velocity. Prisco [26] described the relation between maximized DE and the particle velocity and heat of impact in the cold spray process through a developed mathematical model.

2.3.1. Experiment setup

In this study, the RDE and peak correction factor (PCF) based on experiments are used to characterize the coating profile model under different operation parameters, including spray angle, spray distance and nozzle traverse speed. Experiments were carried out by a homemade cold-spray system, which was equipped with a de-Laval type converging-diverging nozzle. An ABB IRB 2400 robot controls the motion of the spray gun. Therefore, these parameters can be easily controlled by special robot programs. The pure 7075Al powder with a near-spherical morphology was used to coat on Al substrates. The microstructure of powder and the particle size were displayed in Fig.6a and Fig.6b respectively. High-pressure compressed air was used as the propellant gas with a temperature of 550 °C and a pressure of 2.8 MPa. Compressed argon was used as the powder carrier gas. Three groups of tests were carried out: the first one was for testing the effects of spray angle; the second one was for testing the effects of nozzle traverse speed; the third one was for testing the effects of spray distance. Table 1 lists the detailed description of operating parameters. A profile meter (LJ-V7000, Keyence, Japan) was used to measure the individual spray pass thickness after spraying.

2.3.2. Results and discussion

2.3.2.1. Effects of spray angle

In practice, spray angle affects not only the DE but also the shape of the coating-profile. The results of group 1 were measured

and shown in Fig.7. It is realized that the maximum thickness reduces and the asymmetry transforms more obvious with decreasing spray angles. The coating surface roughness was measured after spraying as shown in Table.2. It illustrates that the roughness of coating was different by different spray angle.The weights of the substrate and substrate+coating before and after spraying was measured. The difference between the two measurements is used to calculate the RDE of different spray angles. We assume that the RDE is 100% when the spray angle is 90º. The results are given in ~~Fig. 7~~ Fig. 8. It shows that the RDE decreases with the reducing of spray angle. Especially when the spray angle decreases to 60º, the DE drops sharply. That was because raising the tangential component of the velocity of the particle raises the probability of particles rebounding, and reduces the particles' bonding strength. Similar results can be found in Li [27] and Chen [16] report. A polynomial (degree = 4) was used to get a fit function as $\zeta(\theta 1)$.

Considering $\zeta(\theta 1)$ into the model, it can be seen that the peak of the coating profile as well as the asymmetry changes according to the spray angle obviously, which has a good agreement with the actual situation as shown in ~~Fig. 8~~ Fig. 9.

2.3.2.2 Effects of spray distance

According to the study published [25,28–30], one of the most important factors, which affects the coating formation, is the critical particle velocity. During the Cold Spraying process, the spray distance cannot be ignored, because the acceleration of the particles continues when they exit from the nozzle. Li et al.[31] have also investigated the effects of spray distance on coating deposition property in CS. Van Steenkiste et al.[32] reported the decrease of DE for Al powder as the spray distance varying from 19 to 38 mm. In this study, The RDE for 7075Al powder as the distance changing from 10 to 45mm was studied. It was determined under the situation that the spray distance of 30 mm corresponded to 100%, which is shown in ~~Fig. 9~~ Fig. 10. The DE raises as the spray distance increases and then reduces with further increasing of it. this phenomenon can be explained by the behavior of particle acceleration under different spray distances. A model of cubic was used to get a fit function as $\zeta(s)$. To explain the variation of particle velocity in the function of spray distance.

2.3.2.3 Effects of nozzle traverse speed

Our experimental results of group 3 revealed that the nozzle traverse speed has little effects on DE during cold spraying, which was also reported by Wong [33] with pure Ti powder as well as Chen[16] with 5056Alpowder. However, the increasing of nozzle traverse speed can reduce the maximum of coating thickness, which can be shown in ~~Fig. 10~~ Fig. 11. This is because, under different nozzle traverse speed, the amount of particle deposition is different per unit time. We assume that the PCF equals to 100% when the nozzle traverse speed is 50 mm/s, and the linear fitting function as $\zeta(v)$ can be got for creating the coating thickness model. Until now, the equation of coating-thickness distribution can be expressed as below:

$$\varphi = \zeta(\theta)\zeta(s)\int_0^T (\int \frac{A\zeta(v)}{\sigma\sqrt{2\pi}} e^{-\left(\frac{(x-\mu_x)^2}{2\sigma^2}+\frac{(y-\mu_y)^2}{2\sigma^2}\right)} dxdy)dt \qquad (2)$$

3. Coating Thickness Simulation under RobotStudio™

The process of coating-thickness simulation should be done in combination with the real robot kinematics info, such as tool center point (TCP) speed or the nozzle traverse speed and position so that it could more accurately represent the distribution of coating thickness after spraying. Nowadays, OLP technique enables robot-programming and process simulation in a graphical virtual environment instead of in the site.

RobotStudio™, a powerful off-line programming software developed by Asea Brown Bovrie Ltd (ABB), enables very realistic simulations on robot motion. It makes use of real configuration files and robotic programs identical to those used on the spraying shop. Besides, RobotStudio™ not only has a wealth of features available to users but also provides the interface to develop customized applications. Therefore, it is possible to develop an application program to simulate the deposition of coatings and the distribution of coating- thickness in the framework of RobotStudio™. In this study, an add-in program was developed in C# (programming language of Microsoft ™ Company) and the data exchange with RobotStudio™ is based on API functions provided by RobotStudio™ [34]. The program details are provided in ~~Fig. 11~~ Fig. 12. It is available for users to focus on coating-thickness calculation and simulation in CS process.

The CAD file of the component is needed in the process of coating simulation. The formats of CAD models such as IGES, STL, STEP, ACIS, and ASCII are available in Robotstudio™. After calibration of the component's position and the TCP, the robotic trajectory should be generated according to the operating parameters. In the CS deposition process, operating parameters are classified into several groups as mentioned in published researches: the parameters of the feedstock jet, and various kinematic parameters. They can be controlled directly (scanning step, nozzle traverse speed, spray distance, scanning step, etc.), or indirectly (velocity and temperature of flight particles, etc.).In this study, the kinematic parameters should be well defined, including nozzle traverse speed, projection spray distance, scanning step and so on. Under the assist of RobotStudio™ and the add-in program TST, a simple zigzag path (as shown in ~~Fig. 12a~~ Fig. 13a) was created on a plat substrate for coating thickness simulation.

During the robot path simulation in RobotStudio™, the speed, the position as well as the orientation of the nozzle will change with the robot movement. These signals can be recorded to generate the discrete points on the path for coating thickness simulation. However, the virtual Robotic controller system in RobotStudio™ collects the data every 24 milliseconds. The distance between two collected points is the product of nozzle traverse speed and time step. Table. 3 listed the distance between two discrete points under

different TCP speed. Thus, an appropriate distance is significant for coating simulation. That is because a large distance gives rise to a less accurate outcome and a small one leads to excessive calculation. In this study, the distance between two consecutive points for calculation should not be larger than σ (the standard deviation of coating coating-profile). Therefore, it is necessary to interpolate a certain number of points between two adjacent points if their distance is greater than σ. At the same time, some of the collected points will be deleted because they are superfluous and can lead to the overload of calculation on the deposition simulation. Finally, the remaining points and interpolation points will be used for coating thickness simulation (as illustrated in ~~Fig. 12b~~ Fig. 13 b and ~~Fig. 12c~~ Fig. 13 c).

According to above-obtained discrete points, the program will compute and generate the coating-thickness distribution by using the coating profile model. The effects of DE caused by spray angles, spray distances and traverse speed are taken into account. The result of coating deposition simulation is presented in ~~Fig. 12d~~ Fig. 13d.

For post-processing, there are two ways to characterize the thickness of the simulated coating. By selecting the measurement position, the coating thickness, which is the shortest distance between the measurement position and the substrate, will be automatically calculated and displayed in the graphical virtual environment (see ~~Fig. 14a~~ Fig. 14a). Besides, the thickness of coating is represented by colors and its range is demonstrated by a color bar. The second way is to use a plane with an optional direction to intersect the coating and obtain the cross-sectional profile. After that, the distance from each point on the cross-sectional profile to the substrate is calculated and exported as a text file (see ~~Fig. 13b~~ Fig. 14b).

4. Experiment and simulation

Simulations and experimental verification were carried out to evaluate the predictive capabilities of this newly developed approach. In the experiment, the pure 7075Al powder was used as feedstock to coat on Al substrates in different shapes. One is a plate(84*63*3mm) to verify the thickness model on flat geometries and the other is a workpiece with three grooves to test the shadow effect on this model. High-pressure compressed argon with temperature of 550 °C and pressure of 2.8 MPa was used as the propellant gas. Other operating parameters are listed in Table. 4. In the simulation, the single coating profile model is generated by deciding each variable in equation 2. the values can be obtained through corresponding experiments. After that, the simulation was carried out with the real configuration files, robotic programs and robot kinematic parameters identical to those used on the spraying shop. The detailed results were presented in the following paragraphs.

4.1. Experiment on a flat

The experiment was performed with the same robot program including the same kinematics parameters as predefined in the

simulation is (see ~~Fig. 12~~ Fig. 13). In order to make the coating in the cross-sectional direction easier to observe and compare, a larger scanning step of 3.8 mm is used. Finally, the experimental result has a good correlation with the one of simulation as shown in ~~Fig. 14~~ Fig. 15. For obvious reason, stripes between two tracks can be observed from both experimental and simulation results due to the large scanning step. It also illustrated that good deposition uniformity can be achieved by specifying a scanning step of the corrected distribution, which was also reported by Cai [15] and Chen [16] with pure 5056 Al powder. For the experiment, the cross-section at the middle was measured by using the profile meter. For the simulation, the second way of post-processing illustrated above was used to determine the results of the cross-section shown in Fig.15b. The data obtained was used to make the chart. Finally, the cross-sectional comparison of coating thickness distribution is displayed in ~~Fig. 15~~ Fig. 16. The results of the error analysis are shown in Table.5, which indicates that the simulated coating profile basically fits well with the experimental ones; the average relative error is 6.85%.

4.2. Experiment on a workpiece with shadow effect

As shown in ~~Fig. 16~~ Fig. 17, the geometric model of the workpiece presents three zones in different groove shapes. ~~The depth of the grooves and the slope of the side walls are different, which will cause different shadow effects during cold spraying. The objective of this experiment is to acquire the coating thickness distribution in each zone under the spray angle of 50 degrees and spray distance of 30 mm. The spray path used for deposition is shown in Fig. 17a. The nozzle reciprocated up and down in a single track. During the movement of the nozzle, the two relatively deep grooves are affected by the shadow effect so that some areas are not directly deposited with coating. Besides, the spray angle and distance will change according to the surface of the substrate (as illustrated in Fig. 17b). This will cause sharply change in coating thickness in different positions. According to the results in Fig. 18, we can see that the coating thickness decreased from zone 1 to zone 3. This is because the spray angle decreased while the spray distance increased, as a result, the RDE becomes smaller. The coating thickness of the other zones where the nozzle passed is almost zero because the deposition efficiency almost zero. For obvious reason, there are no coating deposition on the lower end of zone 3 and zone 2. The cross sectional comparisons of coating thickness distribution in each zone are displayed as Fig. 19.~~ The depth of the grooves and the slope of the side walls are different: the first one is 5 mm deep and 68-degree slope; the sencond one is 10 mm deep and 79-degree slope and the third one is 15 mm deep and 82-degree slope. In the experiment, the objective is to measure the coating thickness in each zone under the spray angle of 50 degrees and spray distance of 30 mm. The spray path used for deposition is shown in red in Fig. 18a. The nozzle reciprocated up and down along the red path. In order to illustrate the effect of different zones on the distribution of coatings during spraying, more details were shown in Fig.18b. The trajectory of the nozzle was indicated as purple balls named targets. Red lines were the direction for spraying, also the centerline of the nozzle. The shortest distance of target-substrate was 30mm in the direction of the red line. The change of the distance truly affects the coating DE as above section explained. White balls were

the Intersections of centerline-substrate. It is sure that there will be coating deposition only where the intersection is created. Green arrows were normal of the intersections. It can easy to found that the angle between the normal and the red line was changed along with the movement of the nozzle, which would lead to different spraying angles and different coating depositions.

Fig.19a and Fig.19b shown the results of experiment and simulation respectively. All zone was affected by shadow effects under experiment settings. The coating in each zone was different: zone 1 had the largest coating thickness and the triangular-like profile was formed; the least amount of particles were deposited in Zone 3, so the coating thickness was minimal. This was because the spray angle decreased as well as the spray distance increased, as a result, the RDE became smaller. Besides, there was no obvious coating on the top surface of the substrate because the DE closed to zero. However, the traces washed by the powder particles could be clearly seen. The cross-sectional comparisons of coating thickness distribution in each zone are displayed as Fig. 20. It is known that the physical influence factors of deposition are very complicated during cold spraying. The parallel multiple passes in a single track will lead to the coating having triangular-like profiles. This is because increasing coating height leads to significant decreasing of DE (more than 35% from Kotoban's report [35]) due to the diminishing of effective impact angle between particles and substrate. Obviously, the coating height of zone 1 increased more quickly than others zone owing to its closer spray distance and larger spray angle, which made it the earliest formation of triangular-like profiles (as shown in ~~Fig. 19 a~~ Fig. 20 a). Since the impact of this aspect was not taken into account in the model used in this article, there were large deviations in the simulated results, especially in zone 1. Table.6 listed the results of the error analysis, proving that this method of coating thickness simulation permits convenient prediction of coating thickness in the case of shadow effects. Based on the simulation results, robotic trajectory, operating parameters, and spray strategy can be re-adjusted, like changing the spray angle, setting different nozzle travel speeds, until achieving the desired coating thickness distribution.

5. Conclusions

In this study, a new approach was developed for simulating coating thickness in CS, especially for the prediction of shadow effects. The experiment result shows that this method can provide acceptable results. The evolving geometric 3D model can be easily handled with existing programming and geometric modeling tools, which implies the possibility of a wide application without specific simulation codes. In addition, it can offer accurate profile prediction in the robot programming platform that enables the integration of robot programming with simulation to better control the coating process. However, our current research is still located at the profile geometric simulation. In the future, process physical phenomena, e.g. plastic deformation and energy conversion, will be integrated with this model so as to realize simulation and prediction for coating quality indicators, such as coating porosity. Moreover, It would be applied as an efficient and effective guideline for CS additive manufacturing and repairing.

Acknowledgments

~~The authors thank the support from the China Scholarship Council.~~The author (Hongjian Wu, Xinliang XIE , Meimei LIU) are grateful for the financial support from the China Scholarship Council.

References

[1] A. Moridi, S.M. Hassani-Gangaraj, M. Guagliano, M. Dao, Cold spray coating: review of material systems and future perspectives, Surf. Eng. 30 (2014) 369–395.
[2] H. Assadi, H. Kreye, F. Gärtner, T. Klassen, Cold spraying–A materials perspective, Acta Mater. 116 (2016) 382–407.
[3] S. Yin, Y. Xie, J. Cizek, E.J. Ekoi, T. Hussain, D.P. Dowling, R. Lupoi, Advanced diamond-reinforced metal matrix composites via cold spray: properties and deposition mechanism, Compos. Part B Eng. 113 (2017) 44–54.
[4] A. Astarita, G. Ausanio, L. Boccarusso, U. Prisco, A. Viscusi, Deposition of ferromagnetic particles using a magnetic assisted cold spray process, Int. J. Adv. Manuf. Technol. (2019) 1–8.
[5] S. Yin, P. Cavaliere, B. Aldwell, R. Jenkins, H. Liao, W. Li, R. Lupoi, Cold spray additive manufacturing and repair: Fundamentals and applications, Addit. Manuf. 21 (2018) 628–650.
[6] R. Jenkins, B. Aldwell, S. Yin, S. Chandra, G. Morgan, R. Lupoi, Solid state additive manufacture of highly-reflective Al coatings using cold spray, Opt. Laser Technol. 115 (2019) 251–256.
[7] W. Li, K. Yang, S. Yin, X. Yang, Y. Xu, R. Lupoi, Solid-state additive manufacturing and repairing by cold spraying: A review, J. Mater. Sci. Technol. 34 (2018) 440–457.
[8] J. Pattison, S. Celotto, R. Morgan, M. Bray, W. O'neill, Cold gas dynamic manufacturing: A non-thermal approach to freeform fabrication, Int. J. Mach. Tools Manuf. 47 (2007) 627–634.
[9] A. Sadovoy, Modeling and offline simulation of thermal spray coating process for gas turbine applications, PhD Thesis, Technische Universität, 2014.
[10] S. Deng, Z. Cai, D. Fang, H. Liao, G. Montavon, Application of robot offline programming in thermal spraying, Surf. Coat. Technol. 206 (2012) 3875–3882.
[11] D.Y. Ju, M. Nishida, T. Hanabusa, Simulation of the thermo-mechanical behavior and residual stresses in the spray coating process, J. Mater. Process. Technol. 92 (1999) 243–250.
[12] J. Liu, Y. Wang, H. Li, S. Costil, R. Bolot, Numerical and experimental analysis of thermal and mechanical behavior of NiCrBSi coatings during the plasma spray process, J. Mater. Process. Technol. 249 (2017) 471–478.
[13] S. Duncan, P. Jones, P. Wellstead, A frequency-domain approach to determining the path separation for spray coating, IEEE Trans. Autom. Sci. Eng. 2 (2005) 233–239.
[14] A. Kout, H. Müller, Parameter optimization for spray coating, Adv. Eng. Softw. 40 (2009) 1078–1086.
[15] Z. Cai, S. Deng, H. Liao, C. Zeng, G. Montavon, The effect of spray distance and scanning step on the coating thickness uniformity in cold spray process, J. Therm. Spray Technol. 23 (2014) 354–362.
[16] C. Chen, Y. Xie, C. Verdy, H. Liao, S. Deng, Modelling of coating thickness distribution and its application in offline programming software, Surf. Coat. Technol. 100 (2017) 315–325.
[17] T. Wiederkehr, H. Müller, Acquisition and optimization of three-dimensional spray footprint profiles for coating simulations, J. Therm. Spray Technol. 22 (2013) 1044–1052.
[18] Z. Djurić, P. Grant, An inverse problem in modelling liquid metal spraying, Appl. Math. Model. 27 (2003) 379–396. doi:10.1016/S0307-904X(03)00044-1.
[19] D.A. Stepanenko, Modeling of spraying with time-dependent material feed rate, Appl. Math. Model. 31 (2007) 2564–2576. doi:10.1016/j.apm.2006.10.005.
[20] A. Hansbo, P. Nylén, Models for the simulation of spray deposition and robot motion optimization in thermal spraying of rotating objects, Surf. Coat. Technol. 122 (1999) 191–201. doi:10.1016/S0257-8972(99)00255-8.
[21] C. Chen, Y. Xie, C. Verdy, R. Huang, H. Liao, Z. Ren, S. Deng, Numerical investigation of transient coating build-up and heat transfer in cold spray, Surf. Coat. Technol. 326 (2017) 355–365. doi:10.1016/j.surfcoat.2017.07.069.
[22] D.L. Gilmore, R.C. Dykhuizen, R.A. Neiser, M.F. Smith, T.J. Roemer, Particle velocity and deposition efficiency in the cold spray process, J. Therm. Spray Technol. 8 (1999) 576–582.
[23] H. Assadi, F. Gärtner, T. Klassen, H. Kreye, Comment on 'Adiabatic shear instability is not necessary for adhesion in cold spray,' Scr. Mater. 162 (2019) 512–514. doi:10.1016/j.scriptamat.2018.10.036.
[24] H. Assadi, F. Gärtner, T. Stoltenhoff, H. Kreye, Bonding mechanism in cold gas spraying, Acta Mater. 51 (2003) 4379–4394. doi:10.1016/S1359-6454(03)00274-X.
[25] C.-J. Li, W.-Y. Li, H. Liao, Examination of the critical velocity for deposition of particles in cold spraying, J. Therm. Spray Technol. 15 (2006) 212–222.
[26] U. Prisco, Size-dependent distributions of particle velocity and temperature at impact in the cold-gas dynamic-spray process, J. Mater. Process. Technol. 216 (2015) 302–314.

[27] C.J. Li, W.Y. Li, Y.Y. Wang, H. Fukanuma, Effect of spray angle on deposition characteristics in cold spraying, Therm. Spray. (2003) 91–96.
[28] S. Yin, Q. Liu, H. Liao, X. Wang, Effect of injection pressure on particle acceleration, dispersion and deposition in cold spray, Comput. Mater. Sci. 90 (2014) 7–15.
[29] J.P. Campbell, A. Astarita, A. Viscusi, G.C. Saha. Investigation of strain-hardening characteristics of cold-sprayed Al-Al2O3 coatings: a combined nanoindentation and expanding cavity models approach. Surf. Eng, 2019. DOI: 10.1080/02670844.2019.1620438.
[30] S. Yin, W. Li, B. Song, X. Yan, M. Kuang, Y. Xu, K. Wen, R. Lupoi, Deposition of FeCoNiCrMn high entropy alloy (HEA) coating via cold spraying, J. Mater. Sci. Technol. 35 (2019) 1003–1007. doi:10.1016/j.jmst.2018.12.015.
[31] W.-Y. Li, C. Zhang, X.P. Guo, G. Zhang, H.L. Liao, C.-J. Li, C. Coddet, Effect of standoff distance on coating deposition characteristics in cold spraying, Mater. Des. 29 (2008) 297–304.
[32] T.H. Van Steenkiste, J.R. Smith, R.E. Teets, J.J. Moleski, D.W. Gorkiewicz, R.P. Tison, D.R. Marantz, K.A. Kowalsky, W.L. Riggs II, P.H. Zajchowski, Kinetic spray coatings, Surf. Coat. Technol. 111 (1999) 62–71.
[33] W. Wong, A. Rezaeian, E. Irissou, J.G. Legoux, S. Yue, Cold spray characteristics of commercially pure Ti and Ti-6Al-4V, in: Adv. Mater. Res., Trans Tech Publ, 2010: pp. 639–644.
[34] M. Moradi Dalvand, S. Nahavandi, Teleoperation of ABB industrial robots, Ind. Robot Int. J. 41 (2014) 286–295.
[35] D. Kotoban, S. Grigoriev, A. Okunkova, A. Sova, Influence of a shape of single track on deposition efficiency of 316L stainless steel powder in cold spray, Surf. Coat. Technol. 309 (2017) 951–958.

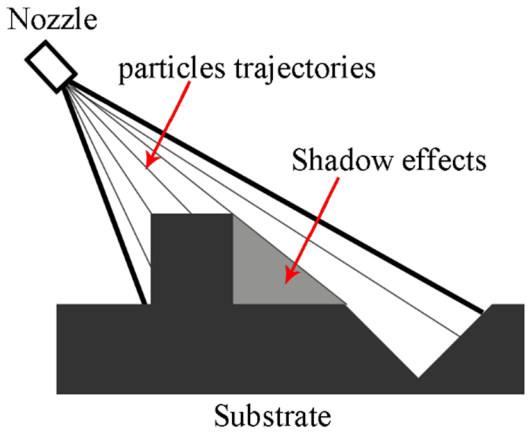

Fig. 1. Coating condition of shadow effect.

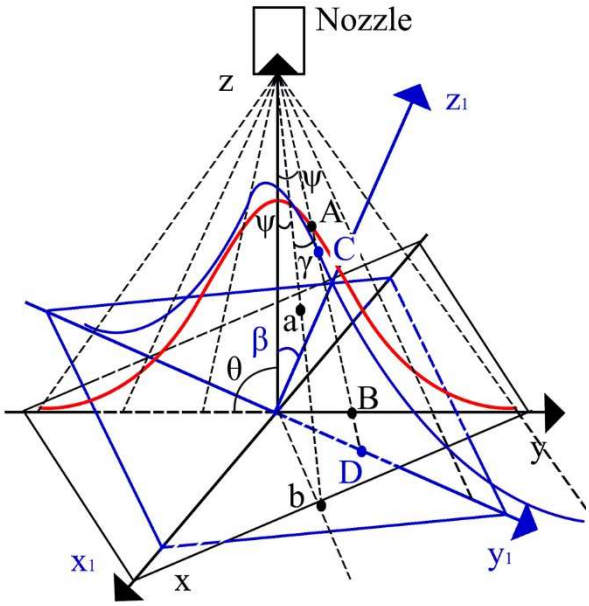

Fig. 2. Schematic of single coating profile model on X-Y plane (red line) and X_1-Y_1 plane (blue line). θ and β are the spray angle on X-Y plane and X_1-Y_1 plane respectively. a is the angle between Z axis and Z_1 axis. ψ is the deflection angle (the angle between Z axis and ab line, as well as AB line). γ is the angle between ab line and AB line.

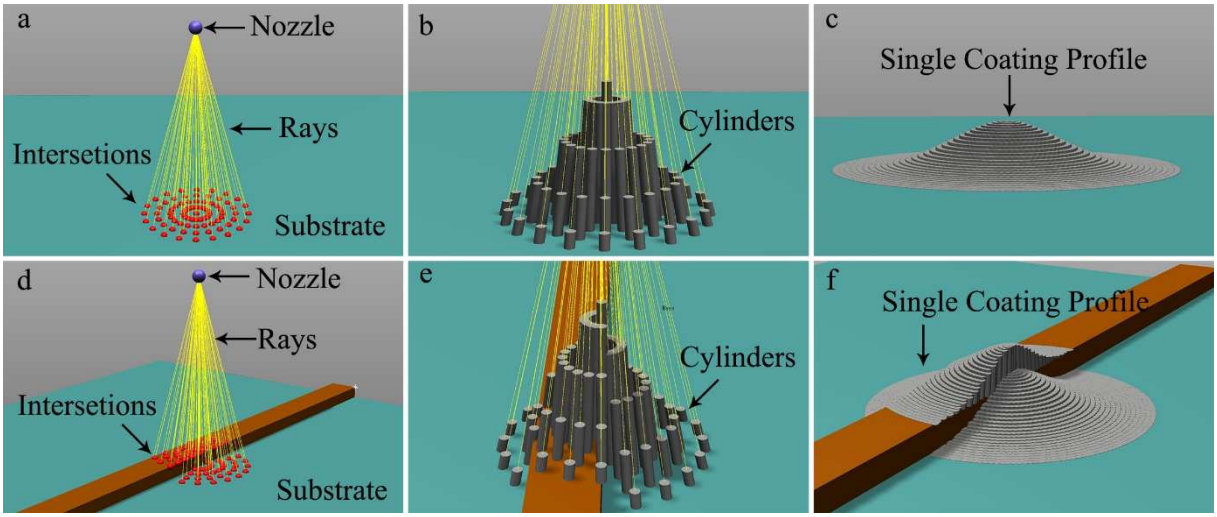

Fig. 3. (a) Create rays and intersection on a flat (b) Create cylinders on a flat; (c) Single coating profile model on a flat; (d) Create rays and intersection on a non-planar; (e) Create cylinders on a non-planar; (f) Single coating profile model on a non-planar;

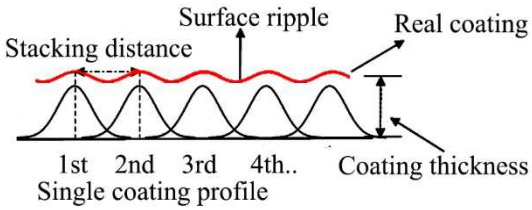

Fig. 4. Schematic of coating thickness distribution model

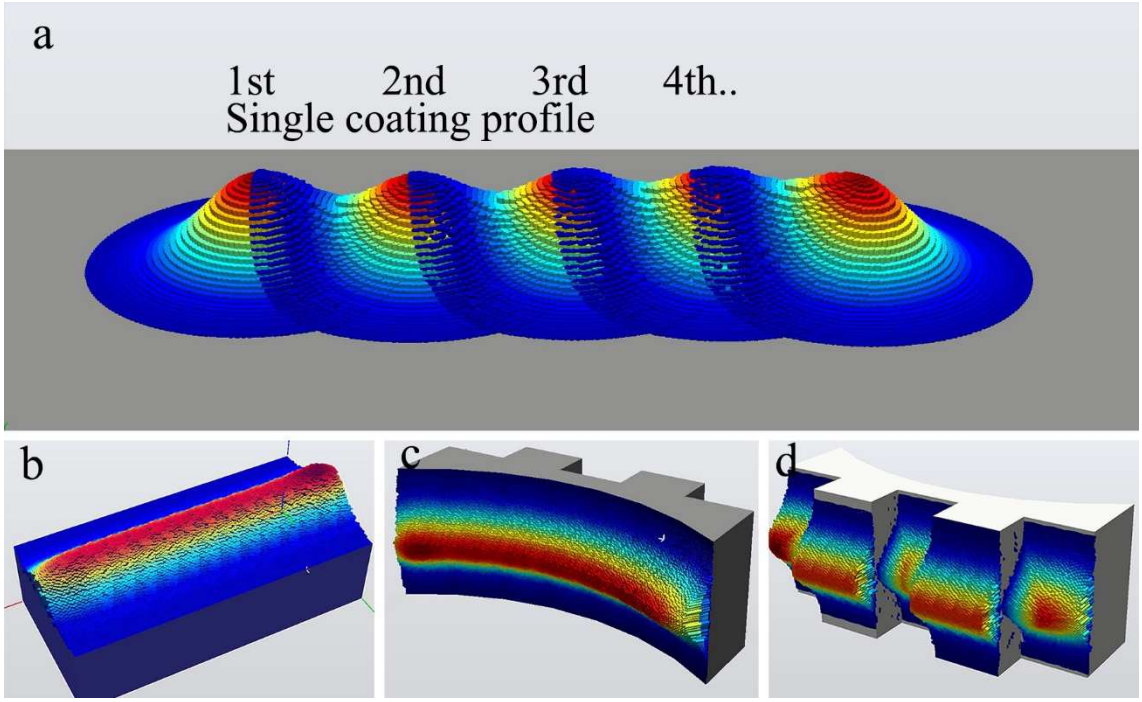

Fig. 5. (a) Discrete single coating profile with overlaps; (b) Continuous single coating profile on a flat; (c) Continuous single coating profile on a curved surface; (d) Continuous single coating profile on a complex surface.;

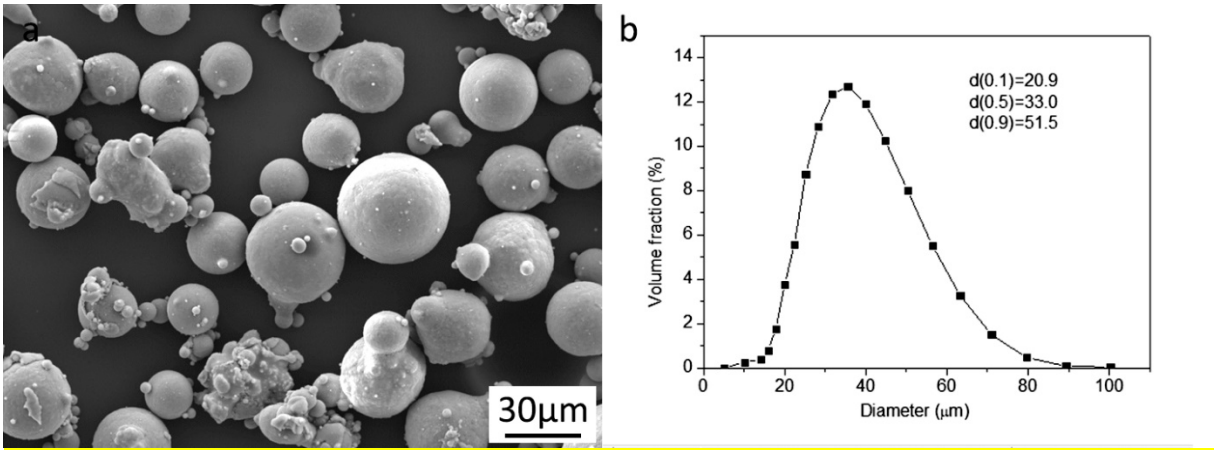

Fig. 6. (a) SEM photos of *Al7075 powder used in experiments* (b) The particles size of *Al7075 powder used in experiments*

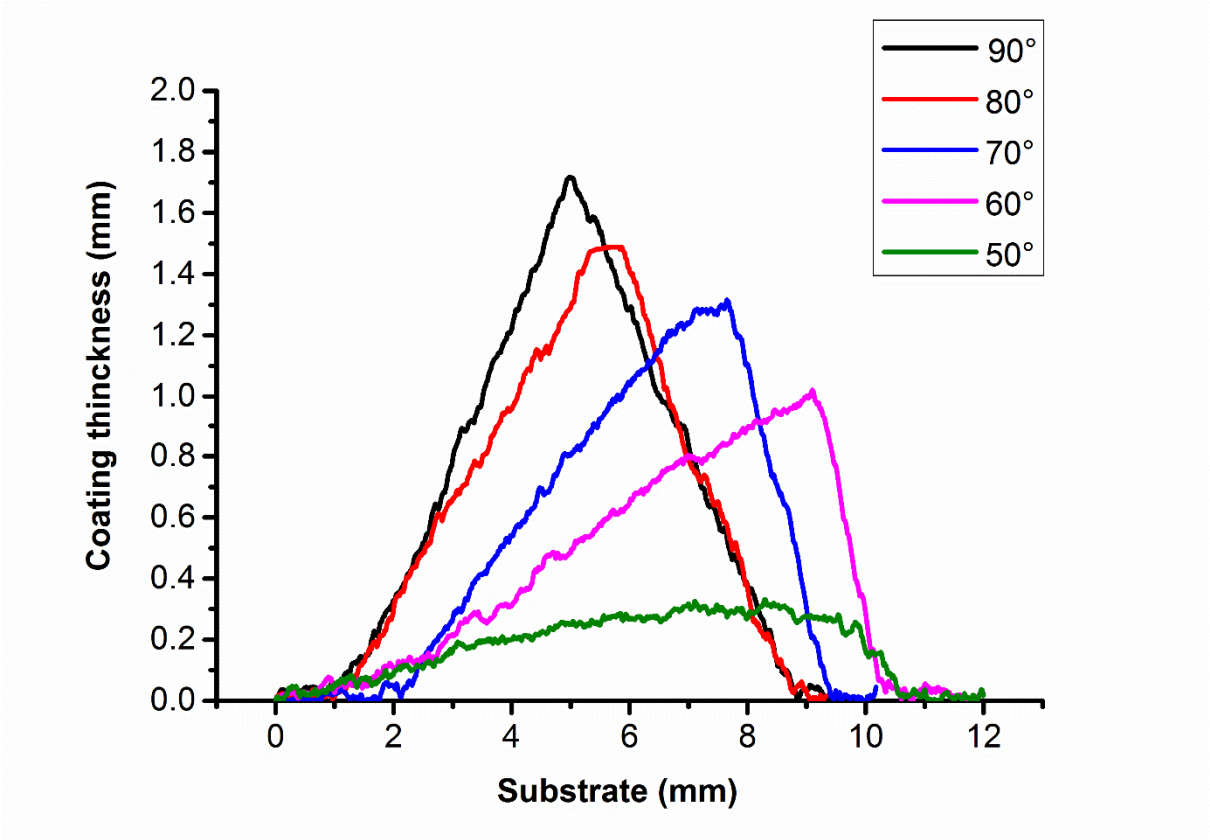

~~**Fig. 6.**~~ **Fig. 7.** The results of coating thickness distribution at spray angle of 90°, 80°, 70°, 60°, 50° respectively.

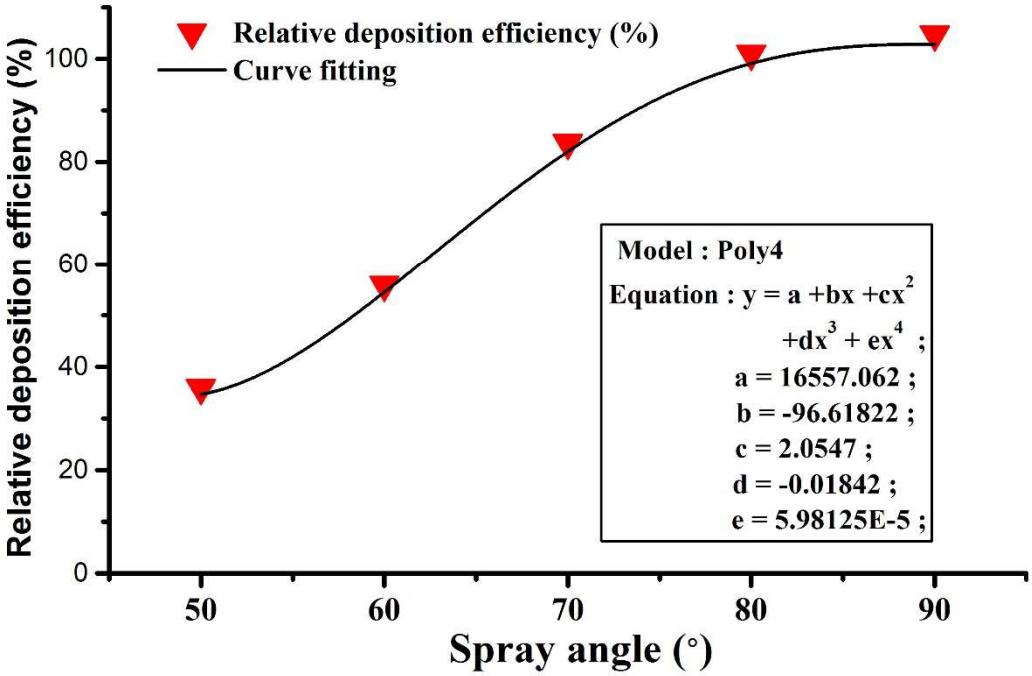

~~Fig. 7.~~ **Fig. 8.** Effects of spray angle on weight gain and relative deposition efficiency of Al7075 coating.

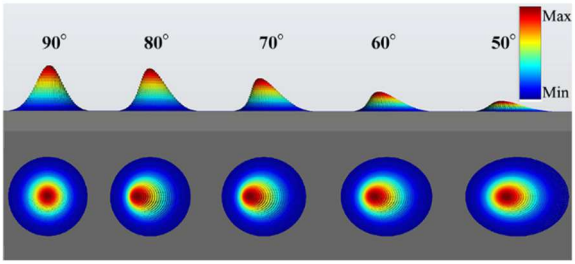

~~Fig. 8.~~ **Fig. 9.** Model of single coating profiles at different spray angles

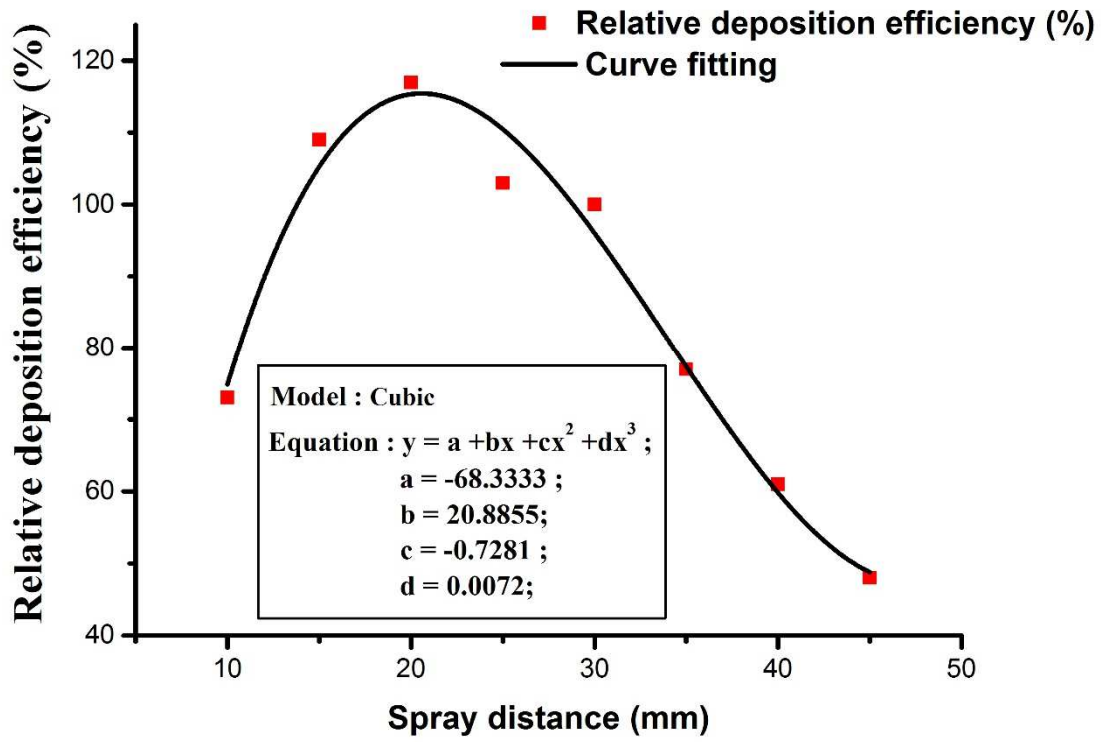

~~Fig. 9.~~ **Fig. 10.** Effects of spray distance (from 10 to 45 mm) on coating thickness and RDE of 7075Al coating.

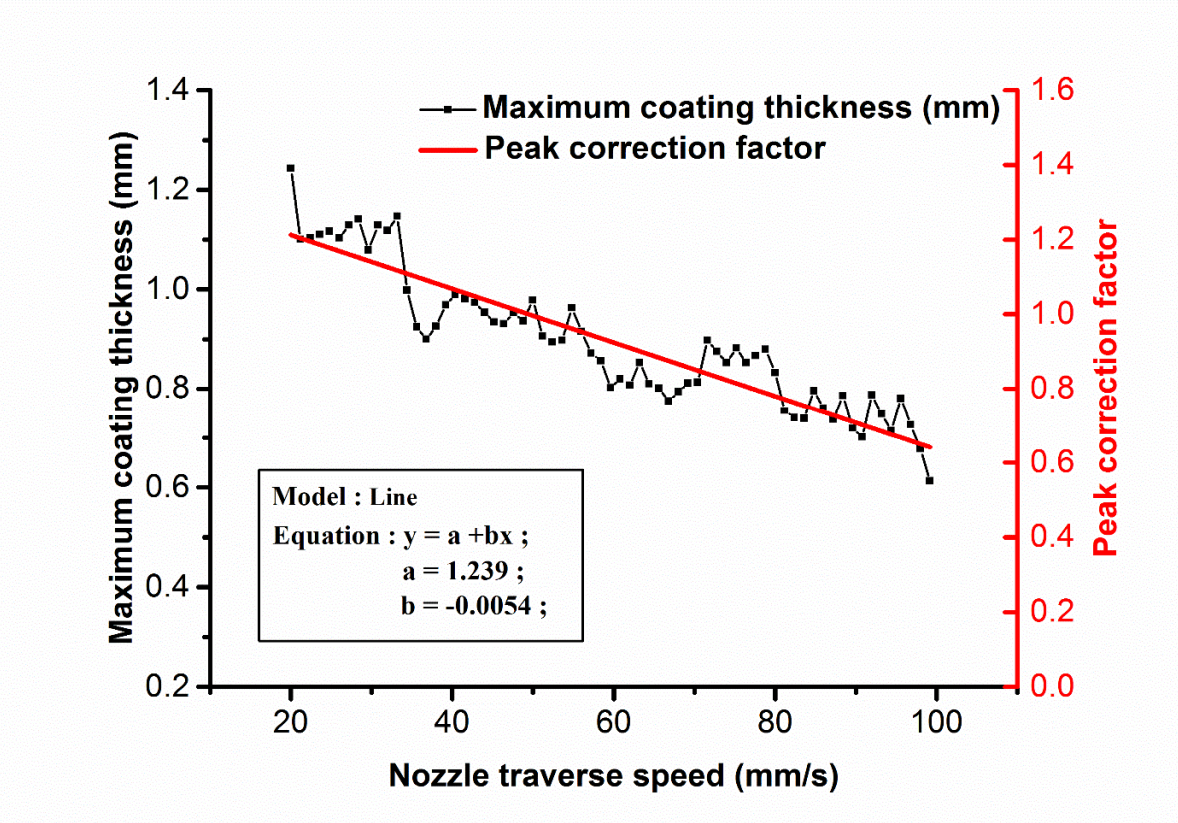

~~Fig. 10.~~ **Fig. 11.** Effects of Nozzle traverse speeds (20~100 mm/s) on coating thickness and peak correction factor of Al7075 coating.

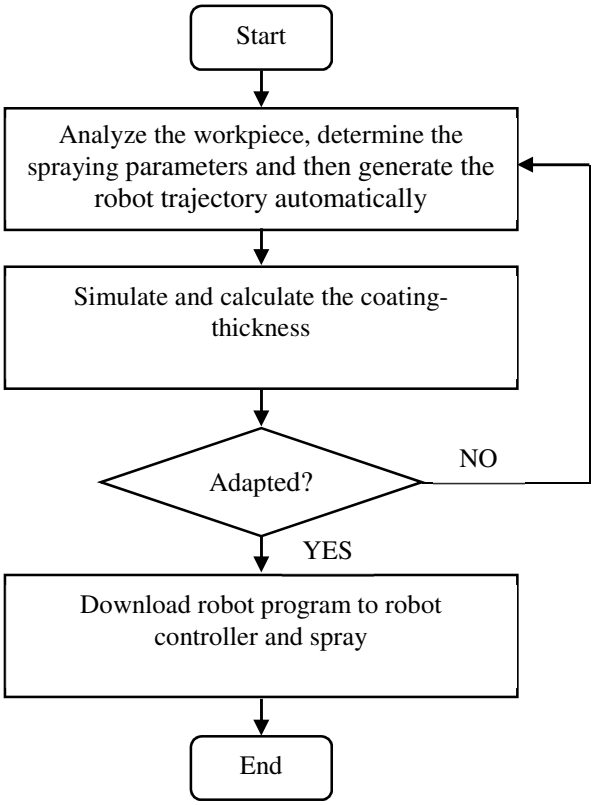

~~**Fig. 11.**~~ **Fig. 12.** Flowchart of the simulation based coating program generation

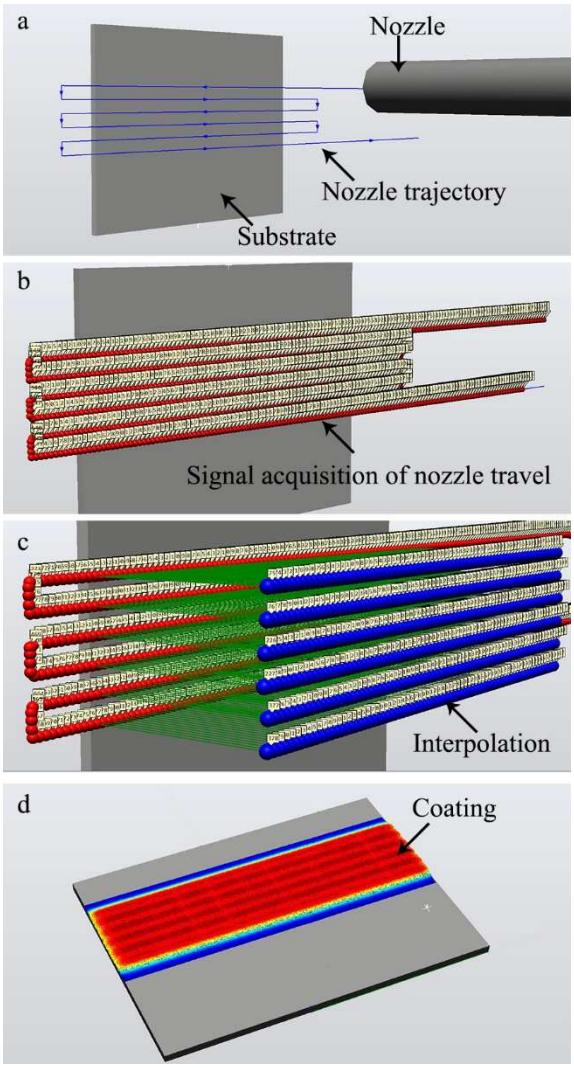

~~Fig. 12.~~ **Fig. 13.** Coating-thickness simulation in RobotStudio™. (a) Generation of trajectory; (b) Signal of nozzle travel; (c) target points for coating thickness simulation; (d) Coating thickness distribution.

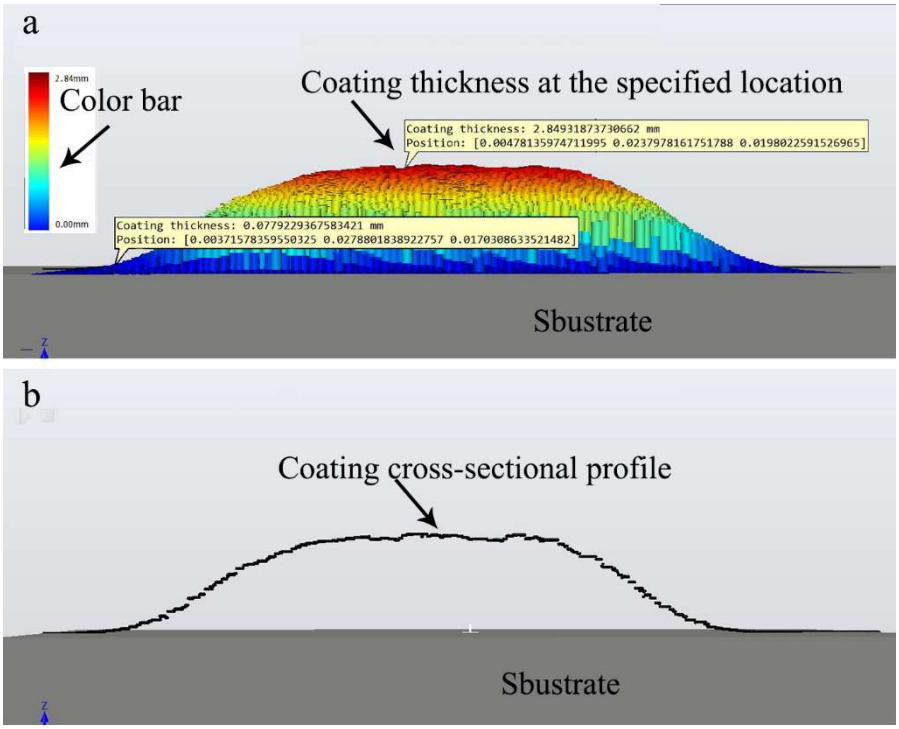

~~Fig. 13.~~ Fig. 14. Calculate and measure coating thickness. (a) Coating thickness at the specified location; (b) Coating cross-sectional profile.

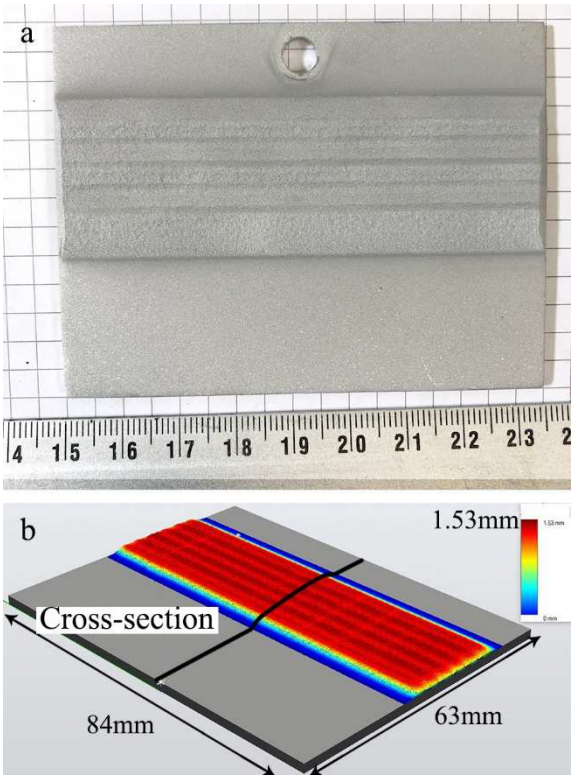

~~Fig. 14.~~ Fig. 15. (a) Experimental result; (b) Simulation result.

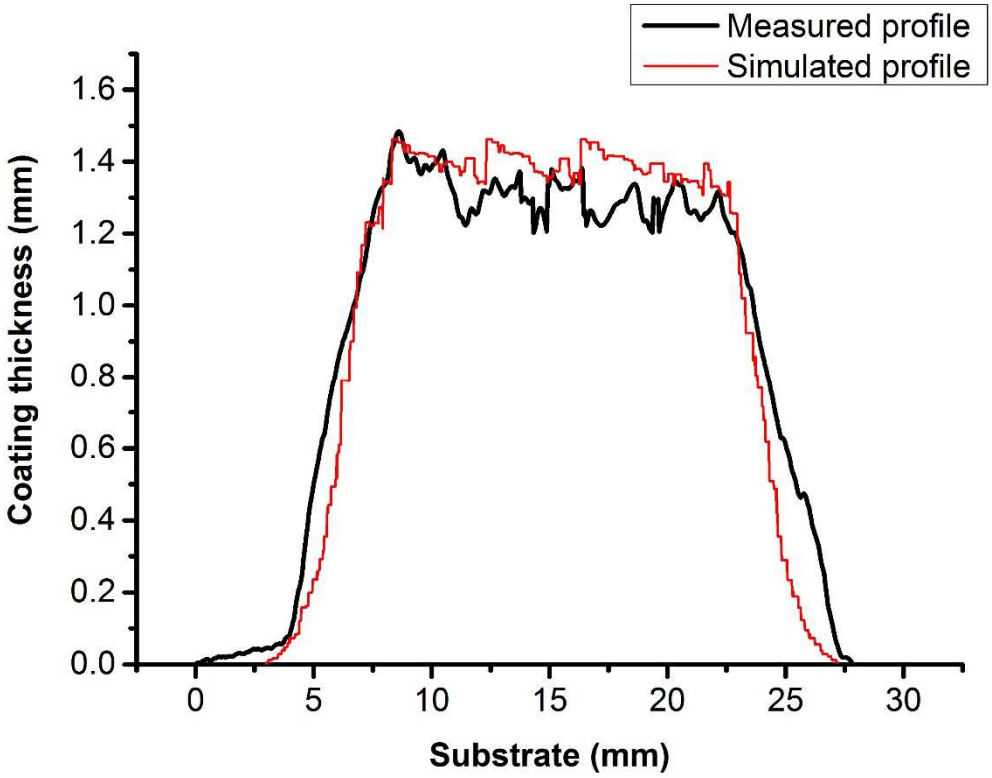

~~Fig. 15.~~ **Fig. 16.** Comparison of experimental and simulation results of coating thickness.

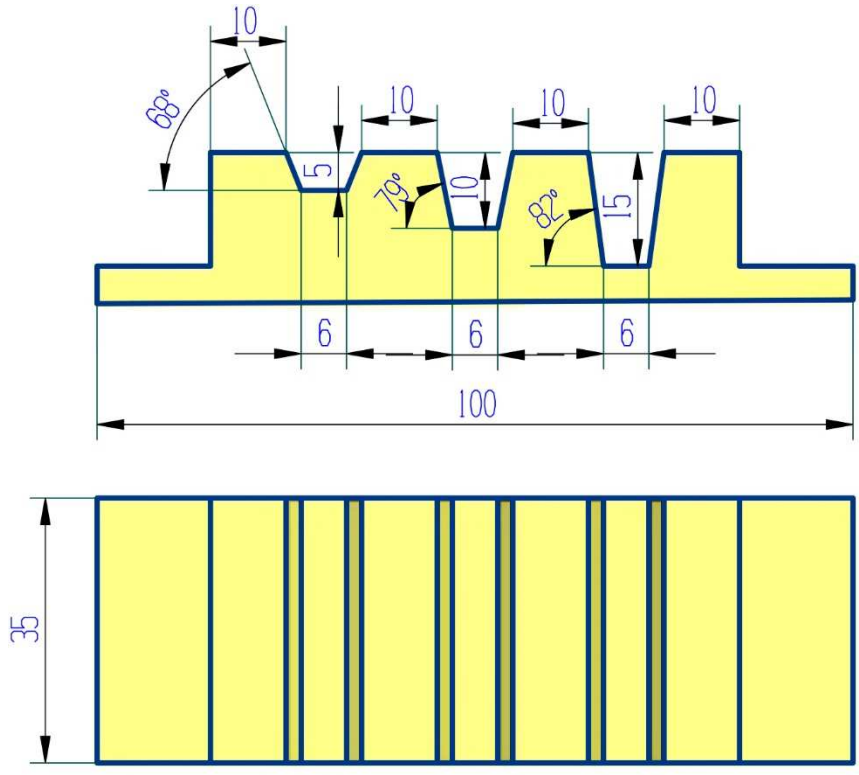

~~Fig. 16.~~ **Fig. 17.** The main view and top view of the workpiece with a shadow effect

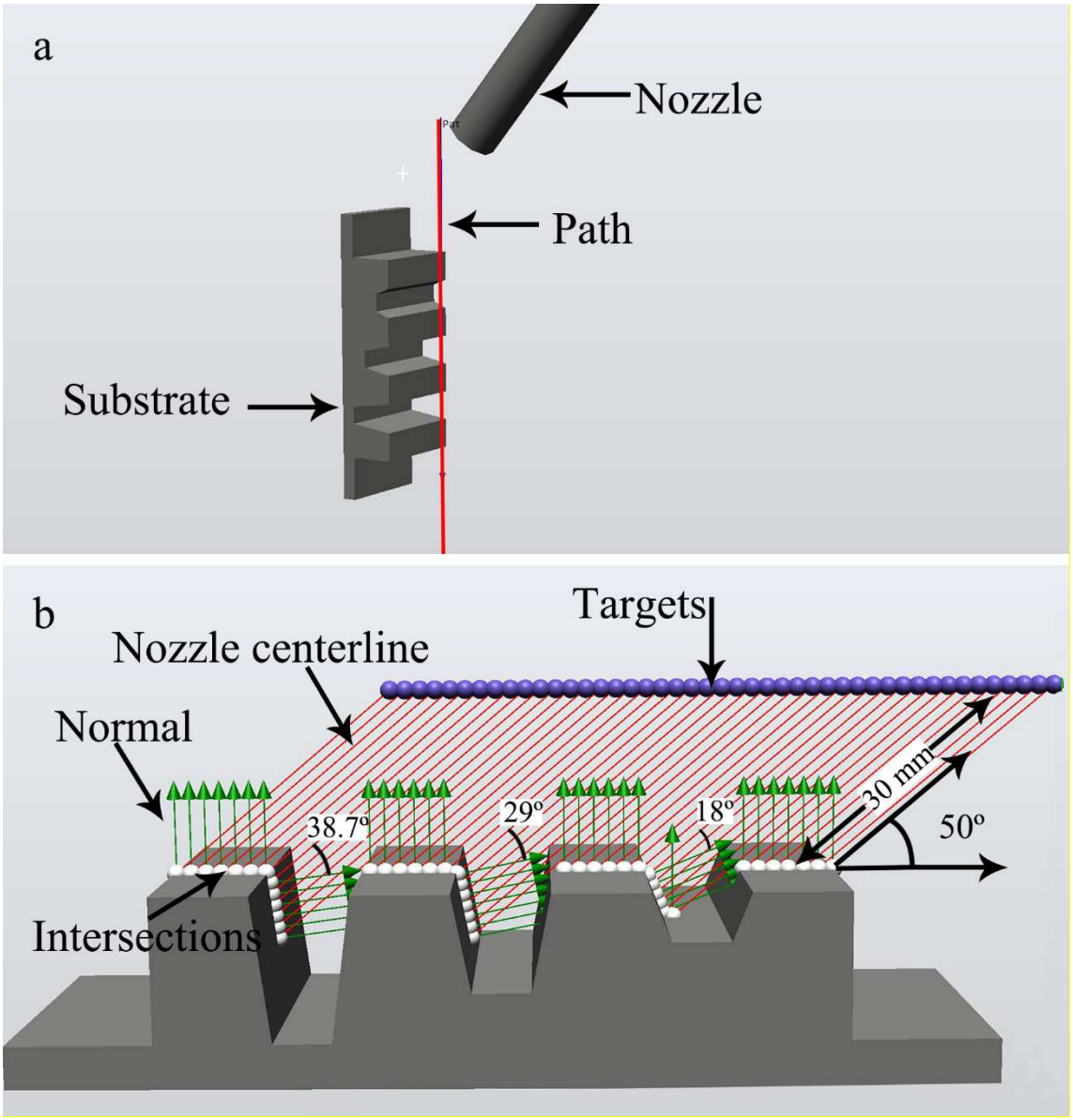

~~Fig. 17.~~ **Fig. 18.** (a) Generation of trajectory; (b) target points for coating thickness simulation.

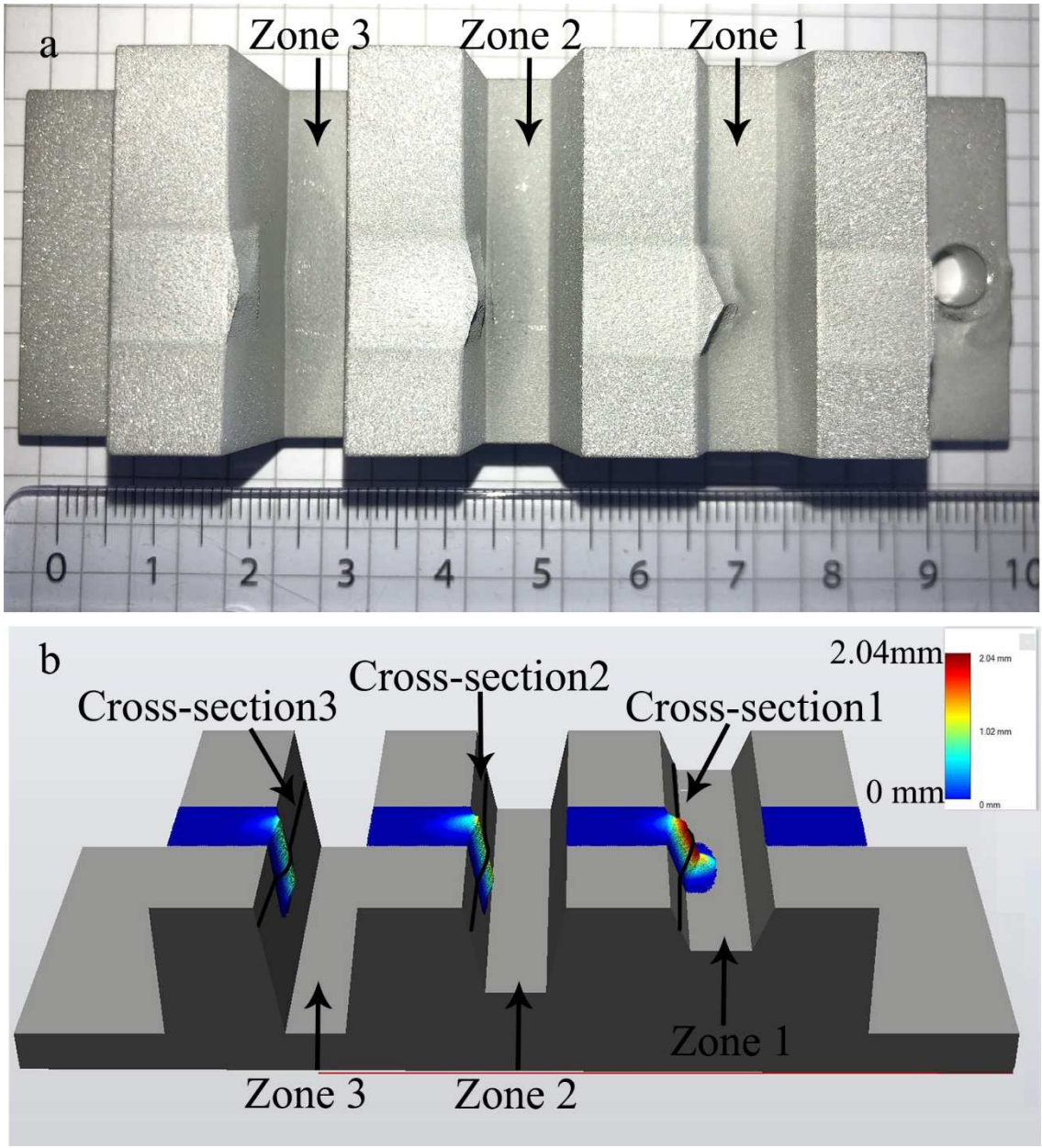

~~Fig. 18.~~ **Fig. 19.** (a) Experimental and (b)simulation results of CS deposition on workpiece with shadow effect.

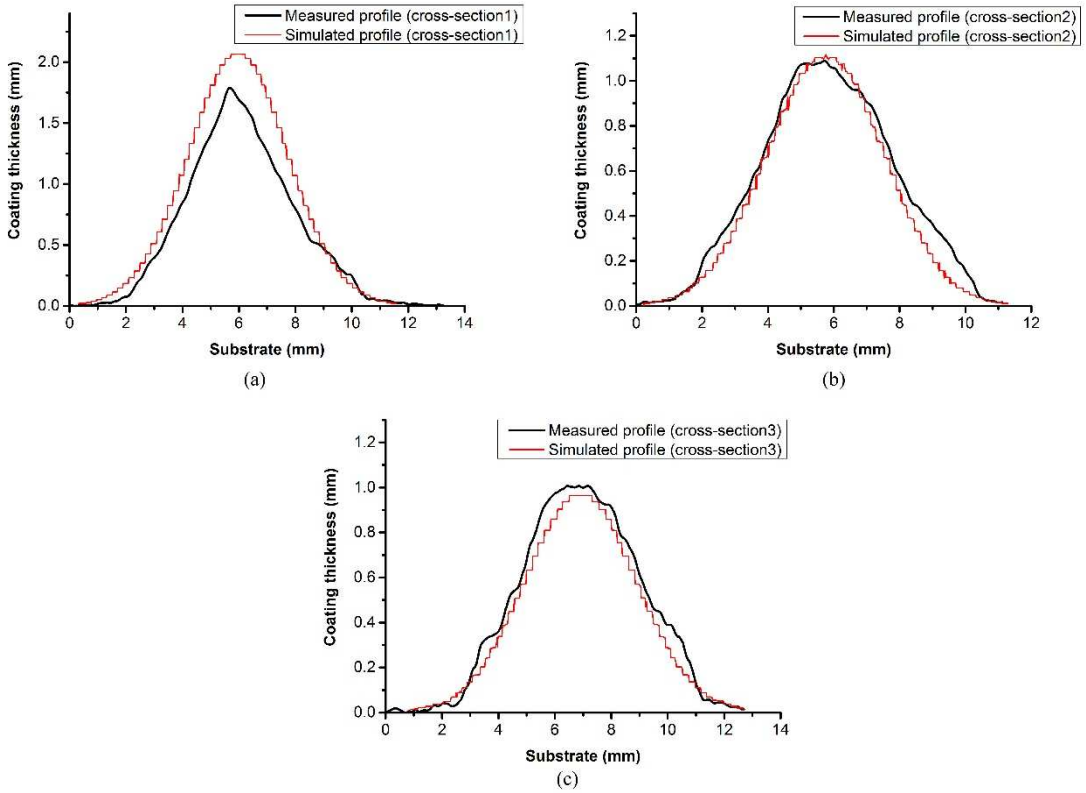

~~**Fig. 19.**~~ **Fig. 20.** Comparison of experimental and simulation results of coating thickness at (a) cross-section 1, (b) cross-section 2 and (c) cross-section 3.

Table. 1. ~~Operating parameter details.~~ Operating parameter details used for effects analysis of the different robot kinematic parameters.

Group	Nozzle traverse speed (mm/s)	Spray angle (°)	Spray distance (mm)	Nozzle pass*
1	50	50-90	30	20
2	20~ 100	90	30	10
3	50	90	10~45	10

*Nozzle pass is the number of times that the nozzle moves along the same track.

Table. 2. The roughness of coatings by different spray angles

Spray angle (°)	Roughness (μm)			Roughness average (μm)
	Test 1	Test 2	Test 3	
90	17.265	16.250	14.467	15.994
80	14.559	18.411	18.140	17.036
70	22.083	18.901	17.933	19.639
60	9.034	17.276	12.049	12.786
50	10.994	11.413	10.964	11.123

~~**Table. 2**~~ **Table. 3.** Distance between two discrete points under different TCP speed

TCP speed (mm/s)	Distance between two discrete points (mm)
1000	24
800	19.2
500	12
200	4.8
100	2.4
50	1.2
20	0.48

~~**Table. 3.** Operating parameter details.~~ **Table. 4.** Operating parameter details used for verification experiments.

Substrate	Nozzle traverse speed (mm/s)	Spray angle (°)	Spray distance (mm)	Scanning step (mm)	Nozzle pass
Flat	50	90	30	3.8	10
Complex	50	50	30	None	20

~~**Table. 4.**~~ **Table. 5.** The average and standard deviation of coating thickness, as well as the absolute and relative error of simulated results with experimental ones.

	Average coating thickness (mm)	Standard deviation (mm)	Average absolute error (mm)	Average relative error (%)
Experiment	1.298	0.056	0.089	6.85
Simulation	1.387	0.044		

~~**Table. 5.**~~ **Table. 6.** The absolute and relative error of simulated results compared with experimental ones base on different cross-sections.

Cross-section	Absolute error (mm)	Relative error (%)
1	0.251	14.03
2	0.025	2.25
3	0.064	6.39